

Article

Simulation Tools for the Architectural Design of Middle-Density Housing Estates

Mathieu Paris ^{1,*}, Marjan Sansen ¹ , Stéphane Bosc ² and Philippe Devillers ^{1,*} 

¹ Laboratoire Innovation Formes Architectures Milieux (LIFAM), Ecole Nationale Supérieure d'Architecture de Montpellier, 34090 Montpellier, France

² Habiter Innover Transformer Laboratoire (HitLab), Ecole Nationale Supérieure d'Architecture de Montpellier, 34090 Montpellier, France

* Correspondence: mathieu.paris@montpellier.archi.fr (M.P.); philippe.devillers@montpellier.archi.fr (P.D.)

Abstract: Temperatures in every Mediterranean city are increasing due to the effects of climate change, with a consequent increase in extreme events. A previous study of French holiday housing designed during the glorious 1930s allowed us to characterize the environmental performance of four additive morphologies. Starting from in situ measurements during a typical summer day and numerical simulations, the goal of this study is to analyze the influence of two calculation methods used in microclimate simulations on the architectural design process. The results are interpreted through the mean radiant temperature and the Physiological Equivalent Temperature, hour by hour in one day, at six different places in a public lane. This work allows us to explore the use of simulation tools for the development of middle-density housing estates to improve outdoor thermal comfort in summertime.

Keywords: architectural and environmental sustainability; urban morphology; urban sprawl sustainability approaches; vegetation; outdoor thermal comfort; Mediterranean climate



Citation: Paris, M.; Sansen, M.; Bosc, S.; Devillers, P. Simulation Tools for the Architectural Design of Middle-Density Housing Estates. *Sustainability* **2022**, *14*, 10696. <https://doi.org/10.3390/su141710696>

Academic Editor: Rajesh Kumar Jyothi

Received: 9 July 2022

Accepted: 16 August 2022

Published: 27 August 2022

Publisher's Note: MDPI stays neutral with regard to jurisdictional claims in published maps and institutional affiliations.



Copyright: © 2022 by the authors. Licensee MDPI, Basel, Switzerland. This article is an open access article distributed under the terms and conditions of the Creative Commons Attribution (CC BY) license (<https://creativecommons.org/licenses/by/4.0/>).

1. Introduction

Languedoc Roussillon, a region that is a part of the French Mediterranean coast, has been one of the most dramatic examples of Urban Sprawl in France, mainly during the period of the 1970s/1990s. In Occitanie, every year, approximately 33 million square meters of natural or agricultural lands are artificialized, making Occitanie one of the regions in France where this process is the strongest. ‘The Explosion of the City’, an international university research study published in 2005 [1], analyzed the different processes that took place in 13 metropolitan regions of Southern Europe (Italy, Spain, Portugal, and France: Marseille and Montpellier). The concept of “Metropolisation of the territory. New territorial hierarchies” was then defined by Francesco Indovina [2], in order to precisely synthesize common trends and local specificities of these Mediterranean metropolitan regions. Dispersion is part of this phenomenon of metropolitan explosion. It took different aspects depending on the region. A key element in the territory of Montpellier, and the region of Occitanie, is the type of housing and, more precisely, the importance of the single-family house. The intensity of the urban sprawl is deeply linked to this type of housing. In most of the towns of the metropolitan area of Montpellier, approximately 80% of housing is single-family houses. For almost three-quarters of the French population (71%), the “villa”, the single-family house, is the ideal accommodation. People usually prefer a location in an urban area and the presence of a garden. This type of housing requires, and generates, important land use, energy, and material demands.

According to the Intergovernmental Science-Policy Platform on Biodiversity and Ecosystem Services (IPBES), 75% of the Earth’s surface is significantly altered. Our impact on the planet is already recorded in geological time, and climate change also bears witness to the entry into the new era of the Anthropocene. The objectives of reducing the artificialization of soils carried by many public policies, particularly in terms of urban sprawl, must

therefore be accompanied by a reflection on the consumption of energy and materials linked to the design and construction, then to the uses that result both from the built morphology but also from the socio-cultural model generated. The urban fabric is a major question of our time. The world's population has doubled in the last 50 years, and more than 55% now live in cities. Economic growth has quadrupled over the past 50 years, increasing the demand for energy and materials exponentially [3]. The Intergovernmental Panel on Climate Change (IPCC) insists, in its latest report, on the importance of mitigation and also adaptation measures. The worst-case scenarios foresee a several-degree increase in the average temperature [4]. The Mediterranean regions will experience extreme hot climatic events in the future and, even if the populations of the countries around the Mediterranean are culturally accustomed to the heat, a reflection on the density and forms of cities must be carried out.

The different processes of urban and architectural transformations of urban and peri-urban spaces must be studied and examined through the prism of climate change, their impact on urban heat islands and outdoor comfort, and their effects on energy demand and the supply of materials. Architects, landscape architects, and town planners must be able to assess the environmental impact of their projects during the preliminary design stages in order to meet the targeted challenges [5]. Terraced houses, semi-detached houses, and patio houses are all alternatives that are useful to consider today and could be possible solutions for the redevelopment of peri-urban areas. We can find interesting cases of alternative habitat morphologies in the architectural experimentations of the 1960s and 1970s, particularly in the frame of the touristic projects of the 'Mission Racine', a French Government Plan from the 1960s for the region of the Languedoc Roussillon, and its touristic development. The 'Grec Village' and 'Ginestous Village' in the city of Leucate (architect: G. Candilis, 1969) or the village of 'Le Merlier, at Cap Camarat (architect: Atelier de Montrouge, 1965) are among these cases, which are sustainable alternatives to sprawl, by the higher density they can represent (Figure 1). Georges Candilis is one of the authors of the coastal development of Languedoc Roussillon. He was a specialist in construction in hot countries. In particular, he led the ATBAT Afrique between 1950 and 1955, and build affordable housing with Michel Ecochard [6], based on the analysis of old Medinas, assembled on the ground floor in an urban frame. The 'Grec Village' can therefore be considered suitable for the warm Mediterranean summer climate.

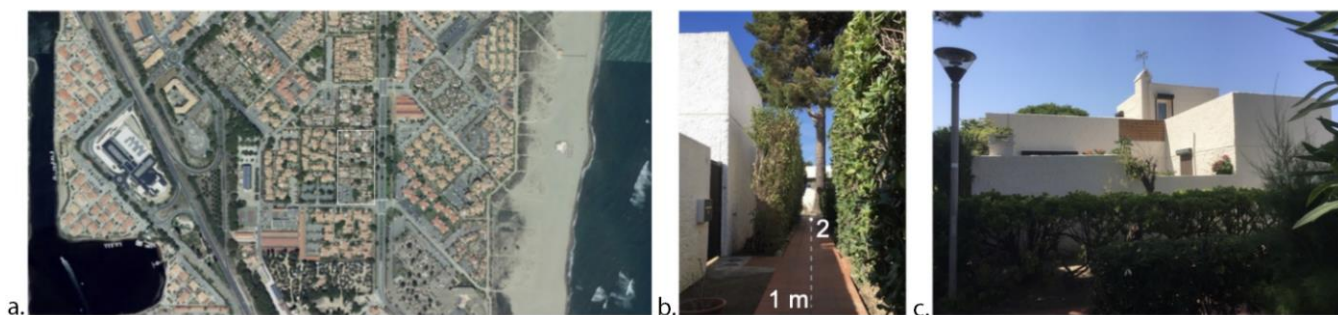


Figure 1. Photography's of the 'Grec Village' in Leucate, France. (a) Aerial view of Leucate; (b) Position of point n° 2 in the study street of the 'Grec Village'; (c) View of a typical 'Grec Village' building.

Today, knowledge on the microclimate issue is mainly based on the historical and dense urban fabric, through the 'urban canyon' and the Sky View Factor. However, these criteria are no longer key issues in suburban areas where density is lower and spaces between buildings are more extended; 'urban canyon' does not really exist there. Urban trees and soil are key elements for the temperature in this kind of urban area. Most of the urban heat islands of suburban areas are located in big parking lots with mineral soil and almost no trees. We know the importance of tree shading and natural soil in the mitigation of urban heat islands. We need to work on the evolution of the usual instruments and tools in order to improve the knowledge of their impact on the evolution of temperatures in

relation to architectural and urban morphology. One of the most significant parameters affecting thermal comfort in the peri-urban environment is the mean radiant temperature (T_{mrt}). The radiative part is important in the perception of external thermal comfort by pedestrians in the Mediterranean climate, as it is necessary to be able to characterize it precisely in order to improve the design of intermediate-density morphologies. Many simulation tools are currently used to estimate the outdoor mean radiant temperature value. This article aims to look at the influence of two calculation methods used in microclimatic simulations on the architectural design process. The first method used in RayMan software is based on the formula of integral measurement of the radiative fluxes defined by Peter Höppe in 1992 [7]. The second method used in Ladybug software consists of weighting the surface temperatures with the corresponding form factors [5]. Starting from in situ measurements during a typical summer day, these two methods are applied to one street of the Grec Village (architect: G. Candilis, 1969) at Leucate. The results of numerical simulations are interpreted through surface temperatures and mean radiant temperatures. Outdoor thermal comfort is analyzed quantitatively through the Physiological Equivalent Temperature (PET) to study the impact of morphology, air temperature, wind velocity, and vegetation. However, the influence of subjective thermal perception is a methodical problem to confirm the accuracy, applicability, and validation of human thermal indices [8]. In the discussion, we will compare the results of simulated PET with those obtained after perceptual readjustment in various studies, notably in Rome in 2015 by Salata [9]. A one-year study involving more than 1000 questionnaires made it possible to determine a neutral PET value in the hot season for this specific place. Finally, we will compare the two simulation methods from the perspective of decision support, the speed of simulation, the interoperability of parameters, the amount of data that can be processed, etc., in order to improve outdoor summer comfort. Recent studies have shown the importance of an architectural design flow integrating microclimatic design parameters from the beginning in order to be able to measure and control the environmental impact [5,10].

2. Materials and Methods

Former research demonstrated that holiday housing is a fundamentally different morphology than a traditional urban downtown morphology [11]. The buildings only have a ground or first floor and are often separated from the street by a courtyard. In addition, the buildings are less compact than in a city center and there is more vegetation. The case study is called the ‘Grec Village’. It constitutes grouped individual holiday housing in Port-Leucate, France (42°51′05.7″ N, 3°02′24.8″ E), and was built in the 1960s by Georges Candilis (Figure 1). The Village is located between the pond and the Mediterranean Sea at an altitude of 4 m (Figure 1). Within the Köppen–Geiger classification, the village has a Csa climate: Mediterranean temperatures with hot dry summers, mild humid winters, and major temperature swings between day and night [12]. Table 1 provides an idea of typical mid-season and summer conditions, with data from the nearby Météo-France weather station in Torreilles. During the summer months, the current mean temperatures are approximately 24 °C, although they reached 39.3 °C in June 2019. Port-Leucate is a very windy site. The main wind directions are NW and SE. Only 5.4% of the time is the wind speed less than 1.4 m/s, and 21% of the time the wind speed is higher than 8.1 m/s. Within the context of global heating, the temperature rise in the case study village could reach 2.4 °C in 2100. This simulation is based on the moderate RCP 4.5 scenario of the last IPCC report [4] and the data of the DRIAS portal.

Table 1. Historical and mean mid-season/summer temperatures (data from Météo-France).

T (°C)	May	June	July	August	September
Max hist.	34.1	39.3	36.9	38.4	36.2
Min hist.	2.9	6.7	11	8	5
Mean	16.8	20.7	23.4	23.2	19.7

The on-site measures were organized on two levels: First, a thermal walk in the morphology, looking for cool spots in order to narrow the research area, followed by street measures in order to characterize the street's microclimate. Compared to typical mean temperatures (Table 1) and winds, the days of the in situ measures were warmer and rather windy (Table 2). A thermal walk, wandering and exploring, allowed us to detect, verify, and confirm the neighborhood's "cool spots". The choice of the streets taken during the walk was inspired by the environmental and typo-morphological analysis of the preliminary work [11]. The street selected was an NS-oriented street. This pedestrian lane is bordered on both sides by high discontinuous hedges (up to 2.5 m). The height of the courtyard walls is shorter than that of the buildings, creating a continuous fabric up to the height of the fence walls and very irregular above (Figure 2).

Table 2. Météo-France's values during on-site street measures.

	T_{\max} (°C)	T_{\min} (°C)	T_{mean} (°C)	Wind Mean Speed (m/s)
22/06/2020	28.9	21	24.7	7.6

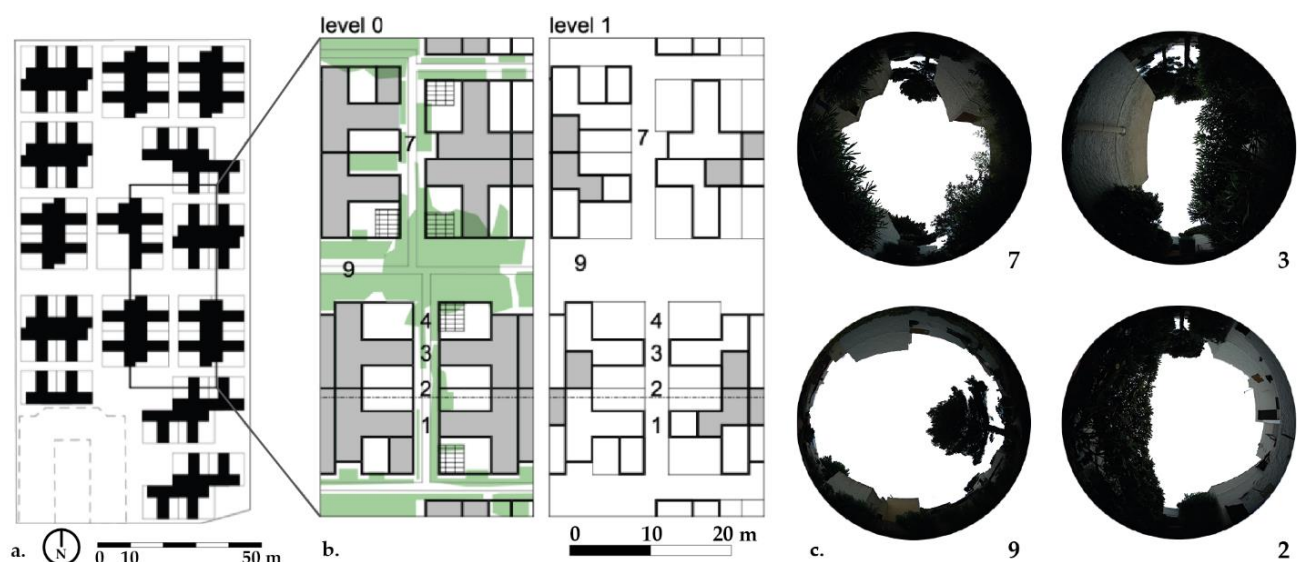


Figure 2. Photographs of the 'Grec Village' in Leucate, France. (a) Plan of the 'Grec Village'; (b) Morphology of the study street and points of interest; (c) Fish-eye photography's of study points.

On a street level, a thermal profile was formulated in the "cool street" one day in summer. This approach was adapted to the scale of the village, performing semi-itinerant measures by foot. For the street-level measures, the temperature, humidity, and mean air speed (Table 3) were monitored every 5 min, at a height of 1 m and in six strategic spots (Figure 2). These were selected concerning different street sections (H/W) and orientations, tree vegetation, and the connection to courtyards (numbers 1, 2, 3, 4, 7, and 9 in Figure 2b). A height of 1 m above ground is similar to humans' meteorologically significant height, or the height of the center of gravity of a standing person according to European standards (≈ 1.1 m) [13]. The experimental device was mounted on a geometer's tripod with a wooden wedge, which allowed us to fix the sensors at the height of 1 m. In addition, photographs were taken to study the built masks thanks to the Sky View Factor (SVF), in the same strategic spots. The SVF photographs were taken with a circular fish-eye lens of 210° on a digital camera, mounted on a tripod at 1 m. The RayMan model is software designed to be run locally on Windows. The model offers estimations of the surface temperature of the ground and the mean radiant temperature (T_{mrt}) at a height of 1.1 m [14]. The model separates the three-dimensional context into two parts: One superior and one inferior. The separation between these two hemispheres is a height of 1.1 m. The lower hemisphere is considered a single solid surface. For this, the albedo must be known

to simulate short- and long-wave radiation flux densities from the ground surfaces. An albedo of 0.34 corresponding to a terracotta tile floor was used for the calculations. For the upper hemisphere, the distribution of built and empty elements was necessary to quantify the radiation fluxes. These data can be obtained using a fish-eye photograph (Figure 2), but when the position of the sun generates rays grazing the edges of the buildings or when the resolution of the images is not sufficient, errors appear and considerably influence the results. The reflection from buildings and trees in the upper hemisphere was not considered, despite the fact that it is an important factor in outdoor thermal comfort. The preliminary study by Sansen [11] on this same case study shows very high perceived temperatures in the patios of the buildings. However, the very high emissivity of the white walls is much less present in the streets where the hedges cast a shadow on the walls. In addition, the air temperature and vapor pressure are required to determine the atmospheric long-wave radiation. The unique surface temperature (T_s) of the lower hemisphere was estimated using air temperature and wind velocity.

Table 3. Technical characteristics of the measuring equipment.

Sensor	Variable	Accuracy	Range	Resolution
Almemo D6	Dry bulb Temp and RH	± 0.3 K ± 1.8 %h	-20 to 80 °C 0 – 100 %	0.01 K 0.1 %h
FVA 615-2	Wind	± 0.5 m/s	0.5 – 50 m/s	0.1 m/s

The RayMan model, which works with fish-eye photos, is an appropriate tool for the simulation of T_s and T_{mrt} , which are essential for thermal comfort simulations. The main advantages of the RayMan software are its ease of use and short operating time compared to other models, which make possible its use by architecture students for their architectural and urban design projects. The Rayman model was therefore adapted to allow an iterative design process, requiring many rapid simulations of different parameters to be useful.

The geometric model that serves as a support for the simulations was developed using the 3D NURBS Rhinoceros 5 modeler. The “Grec village” in the street of interest was modeled through this model with high geometric details (courtyard, hedge, trees, etc.). The urban landscape next to the village was not modelled because the in situ temperature measurements show that the village is not subject to the urban heat island phenomenon (Figure 2), and because the complex air flow pattern was not modelled, real air speed measurements were considered. Surface temperatures of the walls and roofs of buildings, courtyards, vegetation, and soil were simulated using the EnergyPlus simulation engine. The surfaces in the street of interest were modeled so as not to exceed a square of $2\text{ m} \times 2\text{ m}$ and thus ensure a minimum resolution of the variation in surface temperature. In addition, each face of each building was modeled separately. Smaller surface dimensions were retained for the floor in order to separate the different types of floors (terracotta floor, natural floor, and hedges), which are key elements for this type of morphology. In order to calculate a mean radiant temperature, a base long-wave T_{mrt} was calculated using the surface temperatures from the previous step and the formula established by Thorsson [15]. The view factors of all simulated surfaces were determined using the ray tracing function of Rhino’s modeling engine. The long-wave temperature of the sky was calculated using data from the climate file and the formula established by Blazejczyk [16]. To consider the shortwave solar radiation on people, Ladybug Tools’ SolarCalculator model was used to produce an effective radiant field.

3. Results

3.1. On-Site Measures on Street Level

The results are presented Figure 3. The dashed lines correspond to the wind and the solid lines to the temperature. The values obtained correspond to the average temperature over 5 min for each hour between 10 a.m. and 6 p.m. The black arrows correspond to

Météo-France's wind direction and the yellow circles indicate that the sensors were in the sun. The first level of analysis concerns the differences between the data from the meteorological station and the measurements.

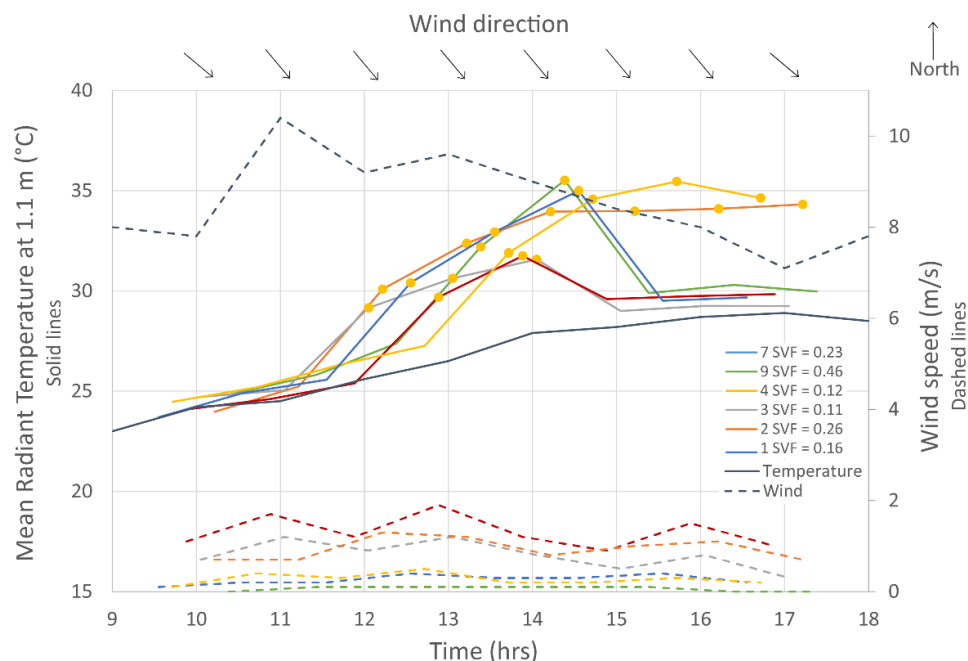


Figure 3. Thermal profile of the street.

The measured wind speeds in the alley are much lower than those given by Météo-France, as the built morphology aptly protects pedestrians from the strong winds typical of the region. There are two reasons for these differences. First, the measurements in the alley were taken at a height of 1 m and an elevation above sea level of 4 m, while the data of Météo-France correspond to a height of 10 m and an elevation above sea level of 42 m. Secondly, the roughness length of the land category can be estimated at approximately 0.5 m considering the built morphology between the pond and the sea, whereas that of the Météo-France data is 0.005 m. The measuring points can be classified into two groups: points 3, 4, and 9 have wind speeds between 0.5 and 1.9 m/s, whereas for points 1, 2, and 7, the wind speed is much lower and less than 0.5 m/s. The points farthest from the main alley with a width of 8 m are those for which the wind speed is the lowest. The differences in wind speed between points 3, 4, and 9 can be explained by the irregularities of the built morphology in terms of height: the implantation of the second floor and the differences in height between the construction's walls and the fence walls.

At the start of the measurements, between 9H30 and 10H30, none of the measuring points were in the sun, and the temperature difference between all the measuring points and the Météo-France data is $\pm 0.5^{\circ}\text{C}$ (Figure 3). This shows that this type of morphology is not subject to the urban heat island phenomenon. During the measurement campaign, the temperature of all measuring points is systematically higher than the Météo-France data. This can be explained by the fact that the Météo-France data correspond to temperatures measured under cover with no radiation, whereas the measuring points, even when not subjected to direct solar radiation, are subjected to diffuse radiation and the radiation emitted from the surrounding surfaces. The coolest spots are points 3 and 4. These points have the smallest SVF and are located on the NS street. The duration of sunshine is between 2 and 3 h, and the wind speed is higher than 0.5 m/s. Point 9 is located in an EO wide street and has the highest SVF. Although the wind speed is higher than 0.5 m/s, it is one of the two warmest spots. For the other points, the wind speed is weak, and the duration of sunshine is between 3 and 5 h. The maximum temperature recorded is higher than 35°C .

(Table 4) and these points are warm spots. Point 2 is one of the most uncomfortable spots. The SVF is the highest in the NS street because of the absence of a hedge on one side.

Table 4. Technical characteristics of the measuring equipment.

Point	1	2	3	4	9	7
Time	14H33	15H43	13H53	14H03	17H13	14H23
T_a (°C)	35.0	35.5	31.8	31.6	34.3	35.5
T_s (°C)	48.6	31.7	43.9	45.8	37.5	47.7
T_{mrt} (°C)	57.1	44.7	54.4	55.3	48.9	56.8
T_{mrt} max (°C)	57.1	56.9	54.4	56.2	54.7	56.8

3.2. Estimation of T_{mrt} with RayMan Software

The mean radiant temperatures have been simulated with the data of the weather station for the relative humidity and the air temperature and with the measured air speed. Choosing the in situ measurement of air velocity rather than the wind speed value of the weather station was dictated by the complexity of the morphology. For the superior hemisphere, the repartition of the solid and free sky elements has been assessed using fish-eye photographs (Figure 2). For the lower hemisphere, the albedo is taken as equal to 0.34, corresponding to the floor covering of the pedestrian lane (terracotta tiles). Between 9H30 and 17H30, the simulated values of the mean radiant temperature vary from 39.7 to 57.5 °C (Figure 4). The maximum simulated values of T_{mrt} are in the same order of magnitude and vary from 54.4 to 57.1 °C. Between 9H30 and 17H30, the maximum simulated values of the surface temperatures vary from 43.9 to 50.7 °C. Two behaviors are observed. For the two spots, 2 and 7, T_{mrt} starts with a high value (52.9 °C), increases slightly, reaches the maximum, and then decreases. For these two spots, T_s is above 40 °C for 63% to 88% of the measuring period. A variation of -18.6 °C of T_s in one hour, even after 5 h at T_s greater than 40 °C, shows that the inertia of the floor covering materials is not considered. For the four other spots, T_{mrt} starts at a moderate value (42 °C), increases, reaches the maximum, and then decreases. What differentiates the four spots is the time during which T_{mrt} remains close to the maximum: only one hour for point 3 and between four to five hours for points 1, 4, and 9.

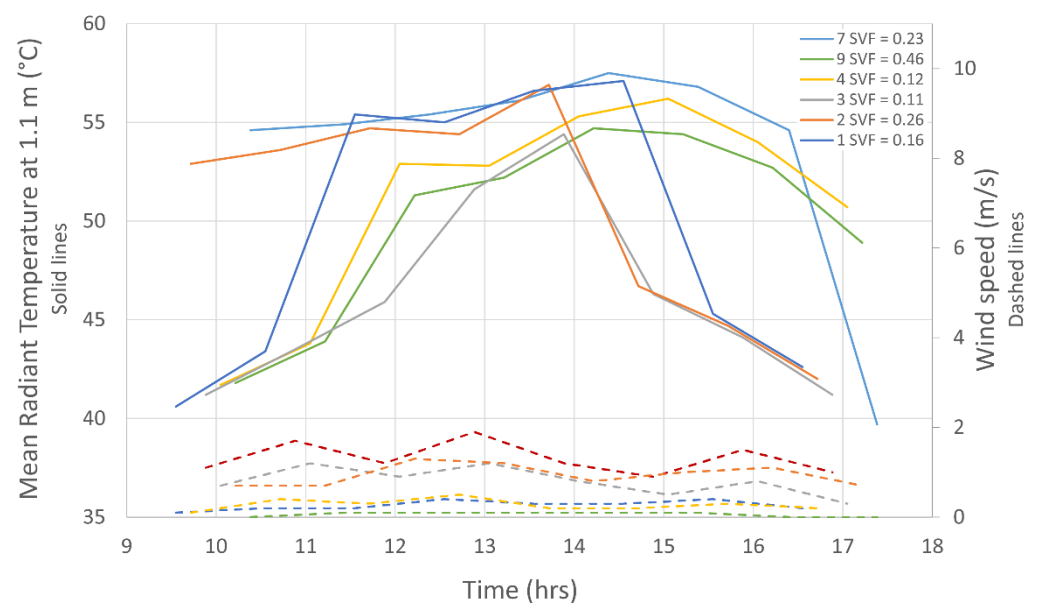


Figure 4. RayMan-calculated mean radiant temperatures.

For the three spots 1, 3, and 7, the maximum mean radiant temperature corresponds to the time at which the maximum air temperature was recorded (Table 4). For spots 2 and 9,

the maximum T_{mrt} occurs between 2 and 3 h before the maximum air temperature was measured. For spot 4, the maximum T_{mrt} occurs 1 h after the maximum air temperature was measured.

3.3. Estimation of T_{mrt} with LadyBug Tools

The surface temperatures of the walls and roofs of buildings, courtyards, vegetation, and soil were simulated using the EnergyPlus simulation engine. Figure 5 shows the temperature of the different surfaces during the simulation at 14H00. In Figure 6, the solid lines correspond to the simulated temperatures with RayMan and the dashed lines to the simulated temperatures with LadyBug. As regards the measuring points, at the start of the study, for spots 2 and 7, the surface temperatures calculated with RayMan are higher than those calculated with EnergyPlus. Then the temperature curves obtained with RayMan are systematically below those obtained with EnergyPlus. The surface temperature curves obtained with EnergyPlus have a much more regular shape, which illustrates the consideration that those computed with EnergyPlus are higher than those computed with RayMan (Table 5). The most important differences are obtained for points 3, 4, and 9, which show a different consideration of the air velocity between the two simulation tools. The time at which the maximum surface temperature was reached is almost identical regardless of the simulation tool used.

In order to calculate the mean radiant temperature for the outdoor comfort estimation, a base longwave T_{mrt} was calculated using the surface temperatures from the previous step for each point. The long-wave temperature of the sky was estimated using the horizontal infrared radiation contained within the climate file. The long-wave temperature of the sky was calculated using data from the climate file. The sky view factors used for the calculation are those obtained with fish-eye photographs because the software cannot consider the hedges, which has the consequence of significantly increasing the values of the sky view factors (Figure 2).

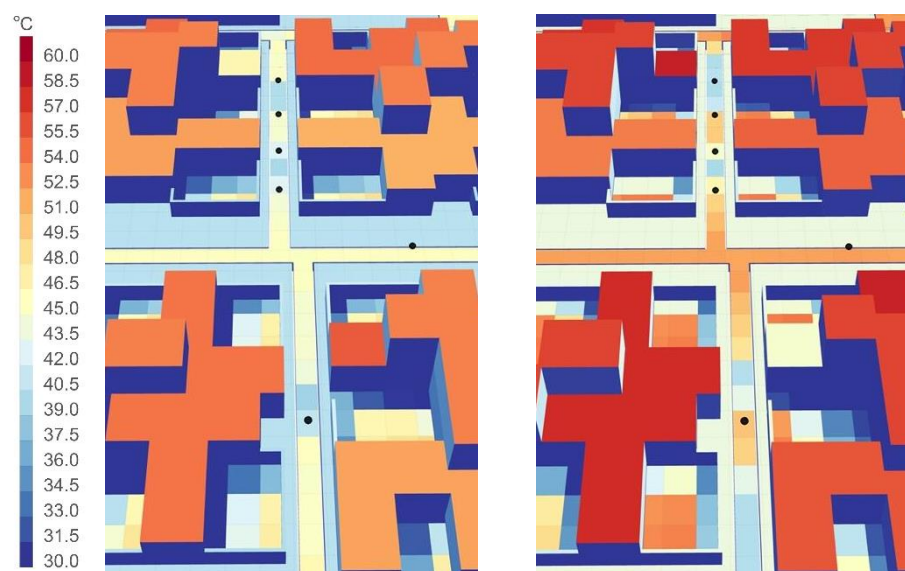


Figure 5. Surface temperatures simulated with LadyBug at 11H00 (left) and 15H00 (right).

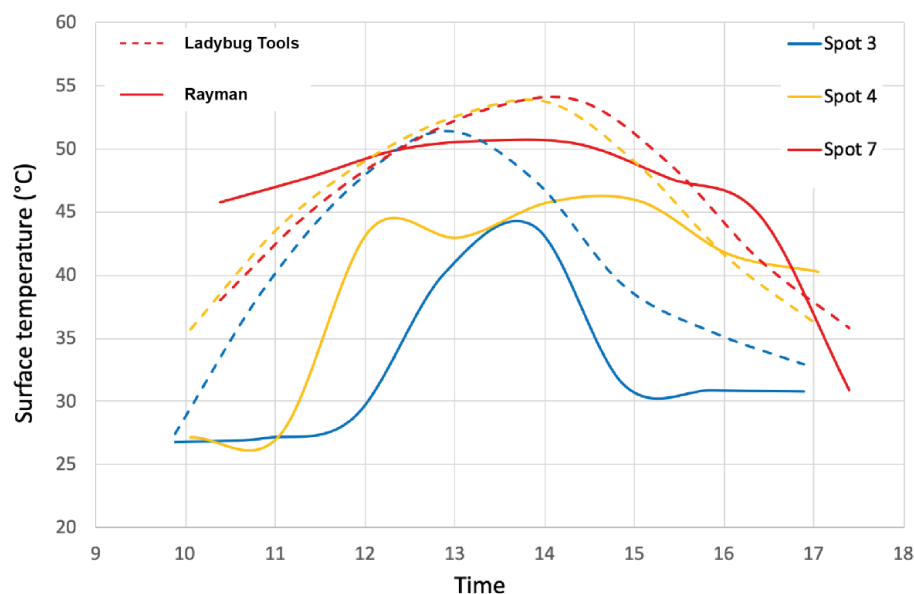


Figure 6. Comparison of surface temperatures simulated with RayMan (solid lines) and LadyBug (dashed lines).

Table 5. Maximum surface temperatures computed with RayMan and LadyBug.

Point		1	2	3	4	9	7
RayMan	T_s (°C)	50.0	50.6	43.9	45.9	45	50.4
	Time	13H33	13H43	13H53	15H03	14H13	13H23
LadyBug	T_s (°C)	51.5	53.9	51.4	53.7	53.61	53.8
	Time	12H33	13H43	12H53	14H03	14H13	14H23

The maximum mean radiant temperatures obtained with LadyBug are systematically higher than those obtained with RayMan (Table 6). The difference varies from +8 °C to +17 °C depending on the spot considered. These differences may be reported at higher surface temperatures for LadyBug than for RayMan. For the two spots 4 and 7, the maximum mean radiant temperature corresponds to the time at which the maximum air temperature was recorded (Table 6). For spots 1, 2, 3, and 9, the maximum T_{mrt} occurs between 1 and 3 h before the maximum air temperature was measured. Considering the mean radiant temperature evolution over the duration of the in situ measurements, the mean radiant temperatures obtained with LadyBug are lower than those obtained with RayMan at the beginning and end of the measurement campaign (Figure 7). At the hottest time of day, the mean radiant temperatures obtained with LadyBug are much higher than those obtained with RayMan.

Table 6. Mean radiant temperatures calculated with LadyBug software at time of maximum temperature recorded on June 22.

Point	1	2	3	4	9	7
Time	14H33	15H43	13H53	14H03	17H13	14H23
T_a (°C)	35.0	35.5	31.8	31.6	34.3	35.5
T_{mrt} (°C)	55.4	47.3	61.3	67.7	56.5	69.9
T_{mrt} max (°C)	65.8	70.1	64.3	67.7	71.8	69.9

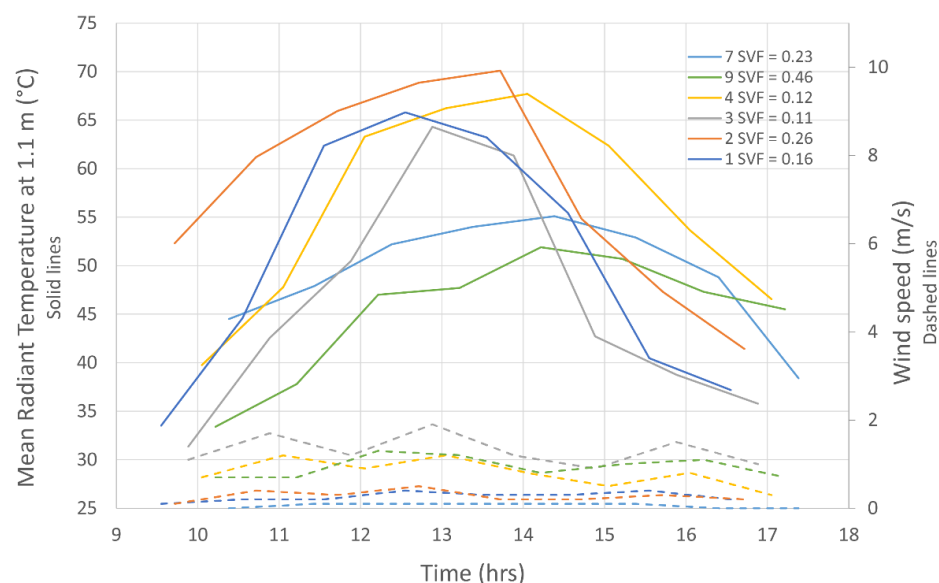


Figure 7. LadyBug-calculated mean radiant temperatures on June 22 between 9 a.m. and 6 p.m.

4. Discussion

The evaluation of thermal comfort of the street has been performed through the Physiologically Equivalent Temperature (PET). Höpfe [17] describes this indicator as the air temperature at which, in an indoor environment where there is no wind or direct solar radiation, the global energy balance of the human body is in equilibrium, with the same overall temperature (internal and skin) as that under complex external conditions. The Physiological Equivalent Temperatures have been calculated for a 35-year-old man weighing 75 kg and measuring 1.75 m. Clothing (clo) has been chosen at 0.5, corresponding to a short skirt, a T-shirt, and sandals. Activity (w) is taken equal to 126 W corresponding to standing with medium activity (Figure 8). In Figure 8, the solid lines correspond to the PET calculated by RayMan and the dashed lines to the PET calculated by LadyBug. The PET values calculated with the two simulation methods have similar tendencies even if those of Ladybug are higher during the hours of direct radiation. The results show the importance of the wind accessibility in the street on the comfort level felt: points 3, 4, and 9, for which the air speed is greater than 0.5 m/s, are the most comfortable points. At no time during the day are points 3 and 9 in the very hot zone, as these are the two points for which the air velocity is the highest (Table 7). On the contrary, point 7, which spends 87.5% of the time in the very hot zone, is the one for which the air velocity is permanently less than 0.1 m/s. Finally, point 3, for which the duration of sunshine is only 2 h, is the most comfortable point. This may be explained by the very irregular layout of the first floors of the ‘Grec Village’: point 3 is the only one that is protected from the sun on the south side by the first floors of the two houses adjoined on each side of the street. In addition, this point is surrounded by two-meter-high hedges on each side of the street (Figure 9). The location of the first floors on the north/west side also allows this point to benefit from good accessibility to the wind.

The difference between the comfort felt during the measurement campaign and the values from the simulations and the PET index may be explained by the computed long-wave mean radiant temperatures starting from the surface temperatures. Indeed, one of the calculation methods, RayMan, does not consider the geometry of the alley and considers it a semi-infinite plane. Considering the width of the lane and the presence of the hedges, the view factor represents 17% of that of a semi-infinite plane. The second method, using LadyBug, considers all the built geometry and its thermal characteristics. However, taking into account the vegetation, in particular the shadow cast on the walls, is not sufficient to obtain consistent results. In addition, several studies in similar climatic zones, such as Rome in Italy by Salata in 2016, or Crete in Greece by Tsitoura in 2014, show neutral

values of PET corrected by the cultural factor between 21.1 and 29.2 °C and 20 and 25 °C, respectively [8]. The thermal perception felt during the survey can therefore be distorted and requires local correction. Tan [18] measured mean radiant temperatures from 40 to 66 °C with a grey globe, in Singapore, on a sunny day on a roof. The obtained values are in the same order of magnitude as those obtained in the literature. In the same time slot, for the same period (July) in Freiburg in a semi-open space, Matzarakis [7] obtained T_{mrt} values between 39 and 68 °C. Under the tree canopy, they obtained values between 31 and 40 °C.

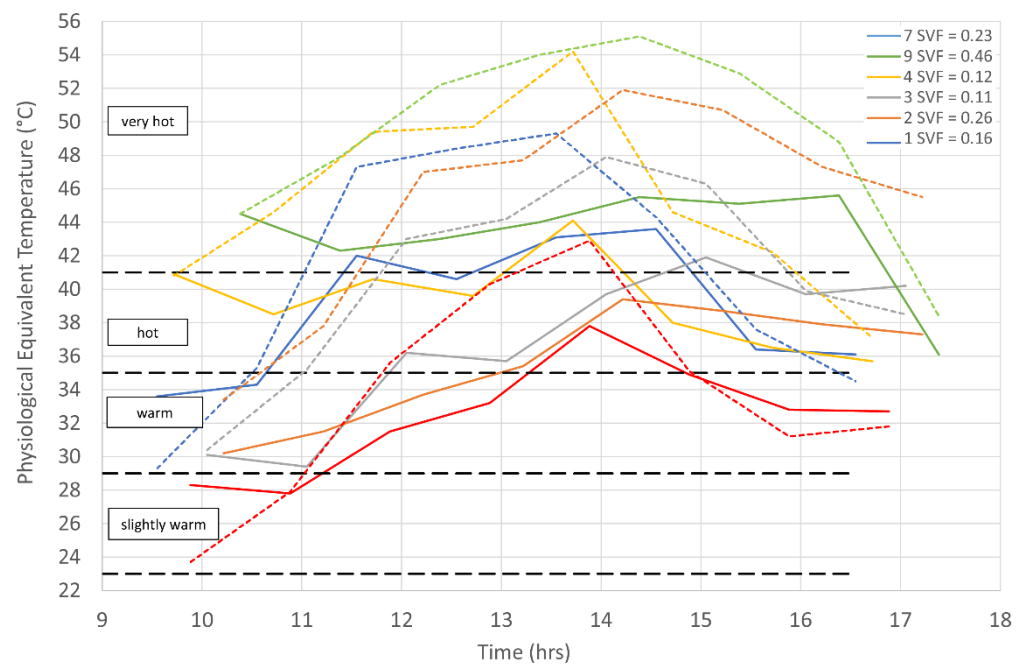


Figure 8. Physiological Equivalent Temperature simulated with RayMan and Ladybug.

Table 7. Percentage of thermal sensation in the street according to RayMan (RM) and LadyBug (LB) during the measurement period.

Point	1		2		3		4		9		7	
	RM	LB	RM	LB	RM	LB	RM	LB	RM	LB	RM	LB
Very hot	37.5	50	12.5	75	0	12.5	12.5	50	0	75	87.5	87.5
Hot	37.5	25	87.5	25	12.5	37.5	62.5	37.5	62.5	12.5	12.5	12.5
Warm	25	25	0	0	62.5	25	25	12.5	37.5	12.5	0	0
Slightly warm	0	0	0	0	25	25	0	0	0	0	0	0

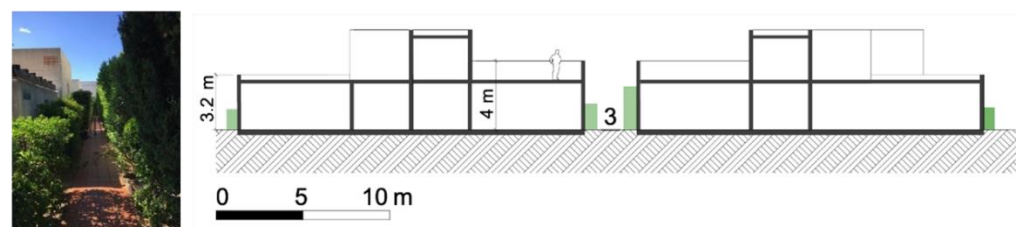


Figure 9. Photography and east/west cross-section of point 3.

RayMan offers the user an instant response obtained only with a fish-eye photo taken on-site or generated and basic climate data. This ease of use leads to errors associated with solid angles, the reflection of materials, and their inertia. In addition, the operability of 3D modeling, simulation, and the reading of results prevent a repetitive iterative process. Ladybug requires longer modeling preparation for surface temperature and T_{mrt}

calculations. This method also requires more computing power. However, the quantity of scenarios capable of being simulated is much greater. Through SolarCal and EnergyPlus, the real consideration of the morphology and its thermal and energy characteristics makes it possible to move closer to reality and understand the mechanisms involved. Ladybug also allows greater interoperability with other simulation tools: Flow of fluids, energy demand, production of renewables, natural lighting, etc. [10]. The objectives of outdoor comfort, consumption of energy and materials, etc., must be achieved in a holistic and interconnected way; the design of the urban space and architectural projects cannot be the addition of successive optimization works [5]. The complexity of this software actually allows for a new design process.

5. Conclusions

Housing represents approximately 40% of artificialized land, so finding sustainable alternatives to free-standing single-family houses is a major goal for architects. Heading towards sustainable environments for cities puts even more emphasis on the very close relationship existing between architectural and urban morphologies, and if we go further, soil and vegetation are also essential in this complex system, which has major impacts on local climates. Several conclusions can be drawn from this study. First, we drew theoretical conclusions for lowering the heat in summer in a medium-density housing estate. From a morphological point of view, access to the wind is a determining parameter in the Mediterranean climate. Then, the solar protection provided by the shadows projected from the building influence the feelings of comfort. The Sky View Factor and the orientation of the street are also decisive. The role of plants is also essential. The shadows of the hedges against the walls of the paths and of the trees prevent the solar radiation from reflecting on the light materials of the buildings. Finally, the urban heat island effect is also conditioned in this case by the flow of the wind and the percentage of vegetal soil. Then, methodological conclusions were drawn on the practice of architectural design. RayMan seems much faster and simpler than Ladybug. However, the complexity of Ladybug allows much better interoperability with software for lighting simulation, wind flow, installation of renewable energy production units, and simulation of energy consumption. This software also makes it possible to dispense with on-site measurements, which are very time-consuming, via the simplification of the urban climate using the Urban Weather Generator. To conclude, the practice of architectural design requires further research on simulation tools, their reliability, and the possibility of mixing different factors responding to today's challenges in the context of climate change.

Author Contributions: Conceptualization and writing, M.P. and M.S.; methodology and software, M.P.; validation, S.B. and P.D.; writing—review and editing, S.B. and P.D.; supervision, P.D. All authors have read and agreed to the published version of the manuscript.

Funding: The authors wish to acknowledge the financial funding provided by FEDER—Région Occitanie for the research project “OEHM - Optimisation Energétique de l'Habitat Méditerranéen”.

Institutional Review Board Statement: Not applicable.

Informed Consent Statement: Not applicable.

Conflicts of Interest: The authors declare no conflict of interest.

Abbreviations

IPCC	Intergovernmental Panel on Climate Change
IPBES	Intergovernmental Science-Policy Platform on Biodiversity and Ecosystem Services
PET	Physiological Equivalent Temperature
RCP	Representative Concentration Pathway
SVF	Sky View Factor
ZAN	Zero Net Artificialization

References

1. FONT, Antonio. *The Explosion of the City*; Colegio de Arquitectos de Cataluña: Barcelona, Spain, 2006; Volume 11, p. 128.
2. INDOVINA, Francesco. The Metropolisation of the Territory. New Territorial Hierarchies. In *The Explosion of the City*; COAC-UPC: Barcelona, Spain, 2004; pp. 20–47.
3. IPBES. *Global Assessment Report on Biodiversity and Ecosystem Services*; IPBES: Bonn, Germany, 2016.
4. IPCC, WORKING GROUP I. *Contribution to the IPCC Fifth Assessment Report Climate Change 2013: The Physical Science Basis*; Intergovernmental Panel on Climate Change: Geneva, Switzerland, 2013.
5. Mauree, D.; Naboni, E.; Coccolo, S.; Perera, A.T.D.; Nik, V.M.; Scartezzini, J.-L. A review of assessment methods for the urban environment and its energy sustainability to guarantee climate adaptation of future cities. *Renew. Sustain. Energy Rev.* **2019**, *112*, 733–746. [[CrossRef](#)]
6. Ecochard, M. Casablanca: Le Roman d'une Ville. Editions de Paris: Paris, France, 1955.
7. Matzarakis, A.; Rutz, F.; Mayer, H. Modelling radiation fluxes in simple and complex environments: Basics of the RayMan model. *Int. J. Biometeorol.* **2010**, *54*, 131–139. [[CrossRef](#)]
8. Potchter, O.; Cohen, P.; Lin, T.-P.; Matzarakis, A. Outdoor human thermal perception in various climates: A comprehensive review of approaches, methods and quantification. *Sci. Total Environ.* **2018**, *631*, 390–406. [[CrossRef](#)]
9. Salata, F.; Golasi, I.; de Lieto Vollaro, R.; de Lieto Vollaro, A. Outdoor thermal comfort in the Mediterranean area. A transversal study in Rome, Italy. *Build. Environ.* **2016**, *96*, 46–61. [[CrossRef](#)]
10. Naboni, E.; Natanian, J.; Brizzi, G.; Florio, P.; Chokhachian, A.; Galanos, T.; Rastogi, P. A digital workflow to quantify regenerative urban design in the context of a changing climate. *Renew. Sustain. Energy Rev.* **2019**, *113*, 109255. [[CrossRef](#)]
11. Sansen, M.; Martínez, A.; Devillers, P. Mediterranean Morphologies in Hot Summer Conditions: Learning from France's "Glorious Thirty" Holiday Housing. *J. Contemp. Urban Aff.* **2021**, *5*, 19–34. [[CrossRef](#)]
12. Eveno, M.; Planchon, O.; Oszwald, J.; Dubreuil, V. Climate change and variability in France from 1951 to 2010: Analysis using the Köppen classification and "annual climate types". *Climatologie* **2016**, *13*, 47–70. [[CrossRef](#)]
13. Matzarakis, A.; Mayer, H.; Iziomon, M.G. Applications of a universal thermal index: Physiological equivalent temperature. *Int. J. Biometeorol.* **1999**, *43*, 76–84. [[CrossRef](#)] [[PubMed](#)]
14. Matzarakis, A.; Rutz, F.; Mayer, H. Modelling radiation fluxes in simple and complex environments—application of the RayMan model. *Int. J. Biometeorol.* **2007**, *51*, 323–334. [[CrossRef](#)] [[PubMed](#)]
15. Thorsson, S.; Lindberg, F.; Eliasson, I.; Holmér, B. Different methods for estimating the mean radiant temperature in an outdoor urban setting. *Int. J. Climatol. J. R. Meteorol. Soc.* **2007**, *27*, 1983–1993. [[CrossRef](#)]
16. Blazejczyk, K. MENEX-mE Man-environment heat exchange model and its applications in bioclimatology. In *Proceedings of the fifth International Conference on Environmental Ergonomics*, Maastricht, The Netherlands, 2–6 November 1992; pp. 142–143.
17. Höppe, P. The physiological equivalent temperature—A universal index for the biometeorological assessment of the thermal environment. *Int. J. Biometeorol.* **1999**, *43*, 71–75. [[CrossRef](#)] [[PubMed](#)]
18. Tan, C.L.; Wong, N.H.; Jusuf, S.K. Outdoor mean radiant temperature estimation in the tropical urban environment. *Build. Environ.* **2013**, *64*, 118–129. [[CrossRef](#)]